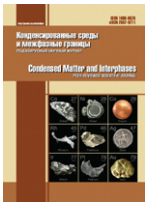

ISSN 1606-867X (Print)
ISSN 2687-0711 (Online)
Condensed Matter and Interphases
Kondensirovannye Sredy i Mezhfaznye Granitsy
https://journals.vsu.ru/kcmf/

Original articles

Research article
https://doi.org/10.17308/kcmf.2026.28/13564

MOCVD and ferromagnetic resonance of epitaxial $Lu_3Fe_5O_{12}$ films for high-frequency applications

A. A. Hafizov[1], M. N. Markelova[1]✉, Gu Ruoxuan[1], I. E. Graboy[1], V. A. Amelichev[2], D. A. Volkov[3,4], D. A. Gabrielyan[3,4], A. R. Safin[3,4], S. A. Nikitov[3], A. R. Kaul[1]

[1]*Lomonosov Moscow State University,*
1. Leninskie Gory, Moscow 119991, Russian Federation

[2]*S-Innovations,*
20-2. Nauchniy Proezd, Moscow117246, Russian Federation

[3]*Kotelnikov Institute of Radio Engineering and Electronics, Russian Academy of Sciences,*
11-7 Mokhovaya st., Moscow 125009, Russian Federation

[4]*National Research University Moscow Power Engineering Institute,*
14-1, Krasnokazarmennaya st., Moscow 111250, Russia

Abstract

Objectives: The production of thin films of rare earth iron garnets with a narrower ferrimagnetic resonance (FMR) linewidth is extremely important in the development of spintronic materials. Among rare earth iron garnets, the compound $Lu_3Fe_5O_{12}$, which has the highest saturation magnetization, is promising. The aim of this work is to study the dependence of the FMR linewidth of $Lu_3Fe_5O_{12}$ iron garnet films on the lattice mismatch between the film and the substrate, as well as on the film thickness during their production by metalorganic chemical vapor deposition (MOCVD).

Experimental: Thin films of $Lu_3Fe_5O_{12}$ garnet were obtained by MOCVD technique on isostructural single-crystal substrates of $Nd_3Ga_5O_{12}$(111), $Gd_3Ga_5O_{12}$(111), $Gd_3Ga_5O_{12}$(210), $Gd_3(AlGa_4)O_{12}$(111) and $Y_3Al_5O_{12}$(111). The films were studied by XRD, EDX, and FMR methods. The dependences of the FMR linewidth on the mismatch of the unit cell (UC) parameters of the garnet at the film–substrate interface, substrate orientation, and film thickness were studied.

Conclusions: It has been established that the minimum FMR linewidth (ΔH) of $Lu_3Fe_5O_{12}$ films is achieved on substrates with minimal mismatch at the interface. The dependence of ΔH on film thickness is shown to be extreme, with the minimum corresponding to a film thickness at which significant relaxation of epitaxial stresses has occurred, but the concentration of defects characteristic of the polycrystalline state is still low. Taking these factors into account will make it possible to obtain iron garnet films with a narrower ferromagnetic resonance linewidth, which can subsequently be used in various areas of spintronics as sensitive elements in microwave detectors.

Keywords: Thin films, Iron garnet, MOCVD, Structure, Ferrimagnetic resonance

Funding: This work was supported by a State assignment to Lomonosov Moscow State University, registration number AAAA-A21-121011590082-2.

For citation: Hafizov A. A., Markelova M. N., Gu R., Graboy I. E., Amelichev V. A., Volkov D. A., Gabrielyan D. A., Safin A. R., Nikitov S. A., Kaul A. R. MOCVD and ferromagnetic resonance of epitaxial $Lu_3Fe_5O_{12}$ films for high-frequency applications. *Condensed Matter and Interphases*. 2026;28(1): 126–136. https://doi.org/10.17308/kcmf.2026.28/13564

Для цитирования: Хафизов А. А., Маркелова М. Н., Гу Ж., Грабой И. Э., Амеличев В. А., Волков Д. А., Габриелян Д. А., Сафин А. Р., Никитов С. А., Кауль А. Р. Синтез из газовой фазы и ферримагнитный резонанс эпитаксиальных пленок $Lu_3Fe_5O_{12}$ для высокочастотных приложений. *Конденсированные среды и межфазные границы*. 2026;28(1): 126–136. https://doi.org/10.17308/kcmf.2026.28/13564

✉ Maria N. Markelova, e-mail: maria.markelova@gmail.com

1. Introduction

The ever-increasing pace of daily data production in a wide variety of human activities, the rapid expansion of accumulated knowledge, and the development of artificial intelligence highlight the fundamental problem of efficient recording and reliable storage of information. This creates significant incentives for the development of new areas of electronics – spintronics and magnonics [1–3]. Spintronic devices are characterized by high write and read speed, information recording density, energy independence, and a number of other advantages over traditional semiconductor electronic analogues [4–6], therefore they have undergone great development over the past two decades. These devices operate using materials in which the primary role is played not by the charge current, which causes Joule heating, but by the spin current, which is free of this drawback. One of the key requirements for such materials is a narrow ferromagnetic resonance (FMR) linewidth [7]. Ferrimagnetic resonance manifests itself in the selective absorption of electromagnetic field energy by a ferrimagnet at frequencies that coincide with the natural precession frequencies of the magnetic moments of the ferrimagnet's electron system in an internal effective field. Intensive research is underway to replace traditional magnetic metals or semiconductors used in spintronic devices with magnetic insulators, specifically ferrimagnetic iron garnets.

The structural type of garnet belongs to the space group *Ia*3*d*. The cubic body-centered unit cell of rare earth (RE) iron garnets consists of 8 identical octants corresponding to the formula composition $\{R\}_3[Fe]_2(Fe)_3O_{12}$, where the curly brackets { } denote the dodecahedral positions of the RE^{3+} ions, and the brackets [ ]- and ( )- correspond to the octahedral and tetrahedral positions occupied by Fe^{3+} ions. The three-sublattice structure and wide possibilities of varying the elemental composition of garnets lead to an almost unlimited variety of their magnetic properties [8].

The narrow ferromagnetic resonance linewidth in iron garnets minimizes losses during electromagnetic wave propagation. A narrower ferromagnetic resonance linewidth in the magnetic layer allows for the propagation of a spin wave or spin current over a greater distance [9], as well as the switching of magnetic moments at a higher speed and with a lower required current density [9, 10]. These arguments indicate that the FMR linewidth is the most important parameter to consider when creating a magnetic layer in spintronic devices. Therefore, producing magnetic iron garnets with a much narrower FMR linewidth than other ferrites and other magnetic insulators has recently become extremely important. For some iron garnet compositions, the width of FMR line is as small as few Oe (e.g., for epitaxial films of $Y_3Fe_5O_{12}$ on $Ga_3Ga_5O_{12}$) [11, 12], while for other compositions the line broadens. At the same time, among RE-iron garnets, there are compositions with high saturation magnetization (e.g., for $Lu_3Fe_5O_{12}$, M_s = 1815 Oe), which is also favorable for the operation of spin devices. The possibility of obtaining thin $Lu_3Fe_5O_{12}$ films with a narrow FMR line would be a significant achievement in expanding the arsenal of spintronic materials, but this requires a detailed understanding of the nature of the FMR line broadening, which is still not fully understood.

The authors of [13] obtained $Lu_3Fe_5O_{12}$ films with a thickness of less than 10 nm on GGG(111) substrates using the molecular beam epitaxy method, in which they showed that $Lu_3Fe_5O_{12}$ films have very low values of the Gilbert damping constant: $11\cdot10^{-4}$ for films with a thickness of 5.3 nm and $32\cdot10^{-4}$ for films of 2.8 nm, which is comparable with the best values of the damping constant for very thin $Y_3Fe_5O_{12}$ films. It is also worth mentioning the discovery of magnetodielectric properties (change in permittivity under the influence of an external magnetic field) in ceramic [14] and thin-film [15] samples of $Lu_3Fe_5O_{12}$. The latter work showed that in epitaxial films of $Lu_3Fe_5O_{12}$ /$Y_3Al_5O_{12}$(111) the magnetodielectric effect at room temperature reaches 0.9 % at a relatively low magnetic field of 1000 Oe and 12.5 % at 9000 Oe. These results indicate the possibility of tuning the magnetic properties of $Lu_3Fe_5O_{12}$ films using an electric field and the real prospects for the subsequent development of microwave modulators, filters, and switches based on them. Recently, Japanese scientists [16] observed the splitting of spin waves

reflected from the edge of the sample into two modes with different wavelengths using doped lutetium iron garnet $Lu_2BiFe_{3.4}Ga_{1.6}O_{12}$ films, which exhibited a much stronger Faraday rotation than $Y_3Fe_5O_{12}$ films. This result demonstrates the potential for controlling spin wave propagation in magnetic films using the modal degree of freedom of elastic waves.

The diverse potential spintronic applications of garnets, and in particular $Lu_3Fe_5O_{12}$, are only just beginning to be realized in operational high-frequency devices [17–19], and for successful development in this area, epitaxial films with a narrow FMR line are primarily needed. Microwave (MW) technology, which has long used garnet films in devices operating on surface magnetostatic waves [20], meets its needs with films obtained by liquid-phase epitaxy, based on growth from supersaturated solution-melts [21, 22]. For applications in spintronics, however, other technological approaches are required to produce thinner epitaxial films (in the submicron thickness range) that are minimally subject to chemical interaction with the melt and the substrate. In light of these requirements, vacuum methods for the epitaxy of RE-iron garnet films are being developed: magnetron deposition [15, 23], pulsed laser deposition [24–26], molecular beam epitaxy [13, 27], and MOCVD [28, 29].

Any film production method involves operational parameters that significantly influence the actual structure and resonance properties of thin films. These parameters influence the simultaneous influence of more general factors that are essential for any film production method and reflect, on the one hand, the principles of epitaxial growth and, on the other, the physics of film magnetism. Given the exceptional sensitivity of resonance properties, developing methods for producing spintronic materials necessitates a detailed study of the role of all factors and the establishment of optimal values for all parameters affecting the resonance of garnet films of specific compositions.

The aim of this study is to investigate the dependence of the FMR linewidth of lutetium iron garnet $Lu_3Fe_5O_{12}$ films on the lattice mismatch between the film and substrate, as well as on the film thickness during metal-organic chemical vapor deposition. Such studies have not been described in the literature and, therefore, represent a significant innovation.

2. Experimental

$Lu_3Fe_5O_{12}$ thin films were deposited by MOCVD on single-crystal $Nd_3Ga_5O_{12}$ (NdGG), $Ga_3Ga_5O_{12}$ (GGG), $Ga_3(AlGa_4)O_{12}$ (GAGG), and $Y_3Al_5O_{12}$ (YAG) substrates with a (111) deposition surface orientation. In some experiments, GGG substrates with a (210) orientation were also used. $Lu(thd)_3$ and $Fe(thd)_3$ dipivaloylmethanates (thd is the 2,2,6,6-tetramethylheptane-3,5-dionate anion) were used as volatile precursors.

The MOCVD setup is shown in Fig. 1. The precursor source is a microcontainer filled with a homogenized mixture of precursor powders. A thin hole is drilled in the bottom of the microcontainer, through which precursor particles can only spill out when the container is vigorously shaken. Shaking is accomplished by periodically oscillating a small magnet placed inside the container in an alternating magnetic field. As a result, microportions of the precursor mixture are periodically fed into the heated evaporator, almost instantly transforming into the vapor phase. The precursor vapors are then transported by a carrier gas (argon) through a hot line into the reactor, where oxidative thermolysis occurs on the surface of the heated substrate, forming the final metal oxide film. The feed rate was 6.8 μmol/min, and the film growth time was 5–90 min. This setup utilizes a "hot-wall reactor," heated by an external furnace, which reduces temperature gradients in the film deposition zone. To prevent the substrates from

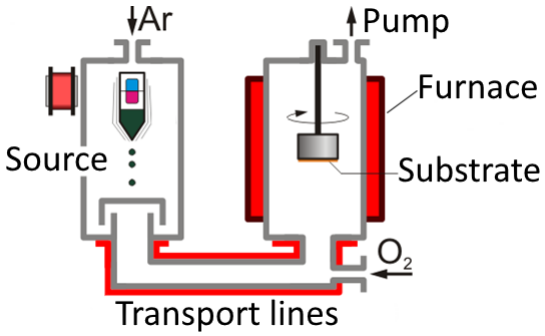

Fig. 1. Schematic diagram of a MOCVD setup with a powder feeder and a hot-wall reactor

being exposed to dusty oxide particles, partially formed when the decomposition of precursors during homogeneous nucleation occurs, an inverted substrate holder was used, to which the substrates were attached from below. In terms of mass transfer, this reactor is a reactor with "stagnant zone", formed under the substrate as a normally directed, rarefied gas flow passes over it. Precursors penetrate from the vapor to the deposition surface via molecular diffusion through a near-surface barrier gas layer, the thickness of which depends on the reactor pressure, the substrate temperature, and the velocity of the incoming gas flow. The hot line and reactor temperatures during deposition were 240 and 970 °C, the total pressure p(total) = 6 mbar, and the partial oxygen pressure pO_2 = 3 mbar. After deposition, the setup was filled with oxygen, and the films were oxidatively annealed at 970°C for 20 minutes. The Fe/Lu ratio in the resulting films was determined using EDX on a Zeiss EVO 50 SEM scanning electron microscope with an e2v Sirius SD IXRF EDMA analyzer. Film thickness was determined from cleavage on a Leo Supra 50 VP scanning electron microscope using a secondary electron detector (SE2).

The phase composition of the resulting films was determined from X-ray θ–2θ scanning data on a Rigaku SmartLab diffractometer (Cu$K\alpha$, secondary graphite radiation monochromator). θ–2θ scanning was performed in the angular range of 5–80° with a step of 0.02°, with a signal accumulation time of 1 s. The ICDD PDF database was used for phase identification. X-ray φ-scanning was used to determine the film orientation in the substrate plane and confirm epitaxial growth. The thickness of the films was determined as follows: two films were analyzed by scanning electron microscopy of a cross-section, their thickness was determined with an accuracy of +/– 5 nm, for the remaining films the thickness was calculated on the assumption that the thickness is directly proportional to the deposition time with constant parameters determining the deposition rate.

To study the ferromagnetic resonance absorption spectra, a setup (Fig. 2) assembled on the basis of a vector network analyzer (VNA), the operating principle of which is described in [17], was used. During the experiments, the real part of the parameter S_{21} was measured for the studied thin-film $Lu_3Fe_5O_{12}$ sample located on a coplanar waveguide. The parameter S_{21} characterizes the ratio of the power transmitted through the coplanar waveguide to the power acting at its input. When the ferromagnetic resonance frequency and the microwave signal frequency applied to the coplanar waveguide input coincide, the microwave signal power is absorbed, which is clearly reflected by this parameter. All obtained dependences of parameter S_{21} were described by a Lorentz function, defining the FMR linewidth.

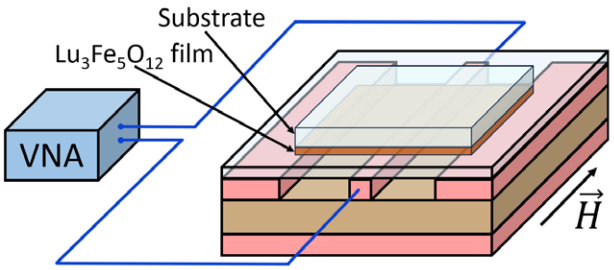

Fig. 2. Schematic diagram of the setup for measuring FMR spectra (VNA – vector network analyzer)

3. Results and discussion

To study the dependence of the FMR linewidth on the substrate type, we selected four substrates with garnet structures: NdGG(111), GGG(111), GAGG(111), and $Y_3Al_5O_{12}$(111) and deposited $Lu_3Fe_5O_{12}$ films of the same thickness (270 nm) on them. All selected substrates are isostructural with each other and with the grown $Lu_3Fe_5O_{12}$ film; however, they have different unit cell parameters (Fig. 3), resulting in different mismatches at the film/substrate interface. The parameter mismatch values (ε) for each substrate/film pair, calculated using the formula:

$$\varepsilon = \frac{a_{\text{film}} - a_{\text{substrate}}}{a_{\text{film}}} \cdot 100\,\%,$$

are 2.3 %, -0.3 %, -0.8 %, and -1.8 % for YAG(111), GAGG(111), GGG(111), and NdGG(111) films, respectively. As can be seen from the calculated values, for YAG, the substrate compresses the film in the contact plane, while for GAGG, GGG, and NdGG, the substrate stretches the film. Thus, during the growth of $Lu_3Fe_5O_{12}$ films on all of these substrates, significant elastic stresses in the film should be expected, which typically lead to

changes in many physical properties, particularly magnetic ones.

As can be seen from the X-ray θ-2θ scanning results (Fig. 4), the films on all four substrates exhibit oriented (444) growth of the $Lu_3Fe_5O_{12}$ phase, mirroring the orientation of the substrates. Considering the X-ray φ-scan results (Fig. 5), which indicate that the film orientation in the lateral plane also follows the substrate orientation, it can be concluded that garnet films on all substrates grow as a single epitaxial "cube-on-cube" pattern. However, alongside reflections from the main garnet phase, the X-ray diffraction patterns also contain peaks from iron(III) oxide and lutetium orthoferrite $LuFeO_3$, the amounts of which do not exceed fractions of a percent relative to the main phase. It is significant that these impurities form only on NdGG(111) and YAG(111) substrates, whose unit cell parameters deviate most from the unit cell parameter of $Lu_3Fe_5O_{12}$. This observation indicates the emergence of obvious difficulties in layer-by-layer epitaxial growth and the facilitation of nucleation of structurally incoherent phases with increasing mismatch of cell parameters at the interface.

By comparing the film peak shifts relative to its position in the X-ray powder diffraction spectrum (i.e., in the free-running, unstressed state), one can assess the presence or absence of an elastic-stressed state, as well as the magnitude of the elastic stress. For example, on GAGG, GGG, and NdGG substrates, a slight shift of the $Lu_3Fe_5O_{12}$ film reflection toward larger angles is observed. This indicates a decrease in the unit cell parameter perpendicular to the substrate due to film stretching by the substrate in the interface plane, while the film's unit cell volume remains unchanged (Table 1). Judging by the insignificant deviation of the film peak from the tabulated value for $Lu_3Fe_5O_{12}$ (444), one can conclude that

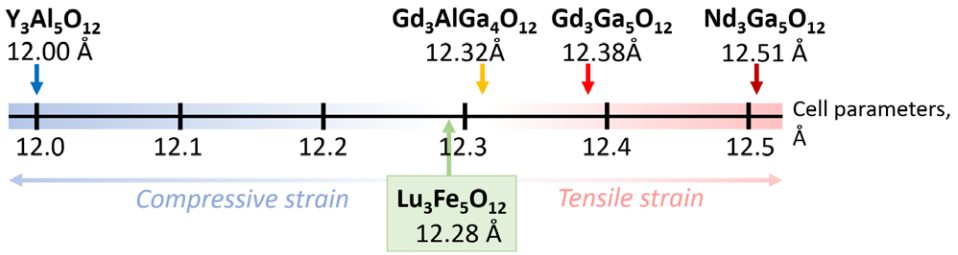

Fig. 3. Schematic illustration of the difference in the unit cell parameters of YAG(111), GAGG(111), GGG(111), and NdGG(111) garnet substrates and $Lu_3Fe_5O_{12}$ film

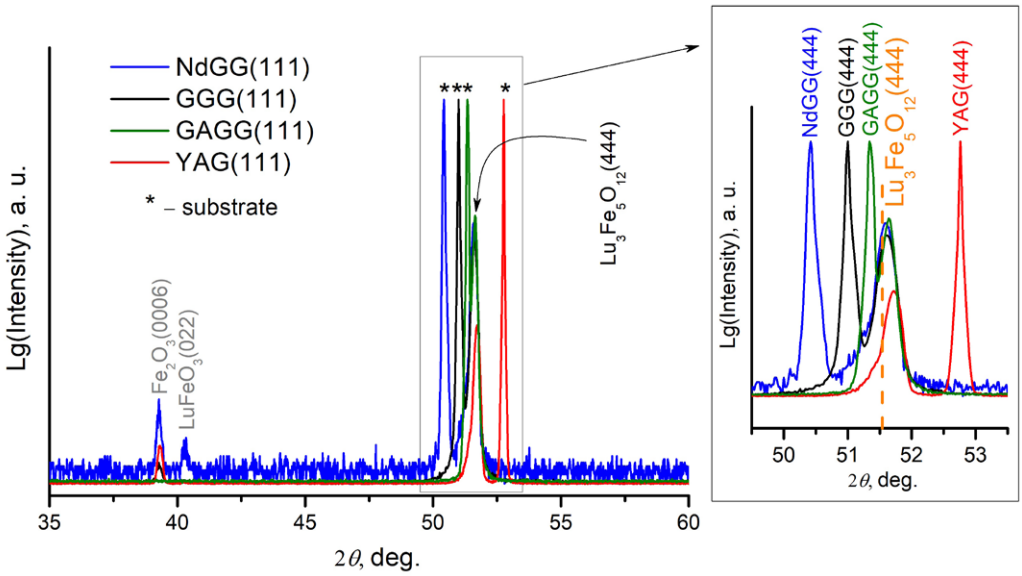

Fig. 4. X-ray diffraction patterns of $Lu_3Fe_5O_{12}$ films deposited on NdGG(111), GGG(111), GAGG(111), and YAG(111) substrates. The dashed line indicates the (444) peak position of bulk $Lu_3Fe_5O_{12}$

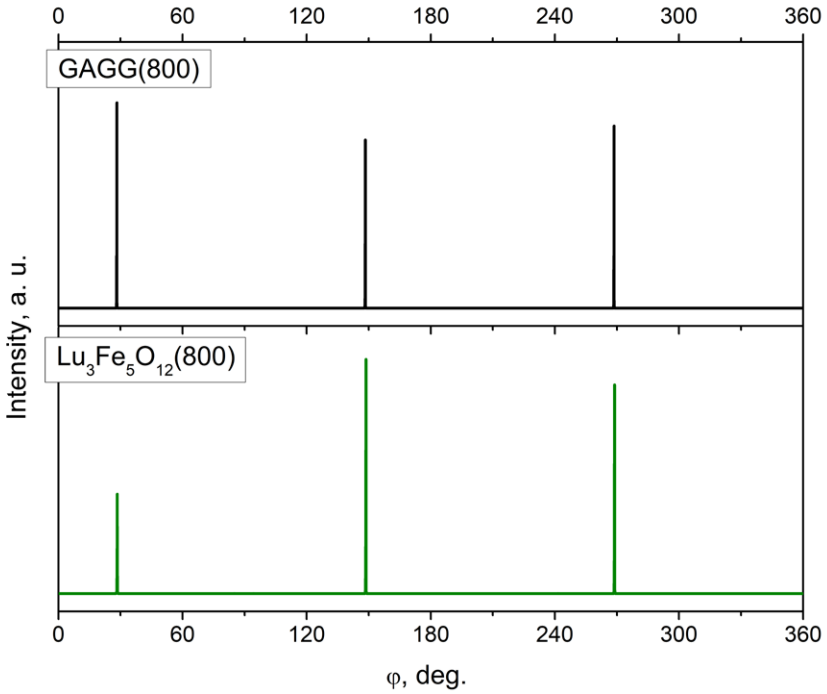

Fig. 5. X-ray φ-scans results for $Lu_3Fe_5O_{12}$ films on a GAGG(111) substrate

the films obtained on GAGG, GGG, and NdGG are in a partially relaxed state. On the YAG substrate, which has a smaller unit cell parameter than the film, a shift of the film peak toward larger angles (i.e., a decrease in the parameter along the normal) is also observed. However, judging by the ratio of the unit cell parameters, elastic stress should cause a deformation of the opposite sign: with the unit cell film volume unchanged, compression along the film/substrate interface leads to an increase in the parameter along the normal to the growth surface and a shift of the film peak toward smaller diffraction angles. The distinct behavior of the $Lu_3Fe_5O_{12}$ film on the YAG substrate suggests that the distortion of the parameters is not due to elastic stresses, but has a different origin. The most likely (but not yet proven) cause is the chemical interaction between the film and the substrate, which involves $Fe^{3+} \leftrightarrow Al^{3+}$ exchange, during which Fe^{3+} ions in octahedral and/or tetrahedral positions are partially replaced by smaller Al^{3+} ions. The possibility of such a substitution was demonstrated in [30] in a study of $Y_3Fe_5O_{12}$ films obtained on $Y_3Al_5O_{12}$ substrates using secondary ion mass spectroscopy. Analysis of the values of the full width at half maximum (FWHM) of X-ray reflections (444) of films on different substrates (Table 1) allows us to state that the most perfect and least stressed epitaxial crystallites of $Lu_3Fe_5O_{12}$ are formed on GAGG substrates.

As shown by the FMR spectral results (Fig. 6a), films on the NdGG substrate exhibit a broader FMR peak compared to films on GGG and GAGG, which is clearly related to the higher stress state of the film on NdGG. It should be noted that at a frequency of 9 GHz, the FMR spectrum of the film on the YAG substrate has a diffuse, weakly

Table 1. Values of unit cell parameters in the direction perpendicular to the substrate (out-of-plane) of $Lu_3Fe_5O_{12}$ films (for comparison, the unit cell parameter for a $Lu_3Fe_5O_{12}$ single crystal = 12.284 Å) and the full width at half maximum (FWHM) of X-ray reflections (444) of films on different substrates

Monocrystal substrate	Out-of-plane unit cell parameter $Lu_3Fe_5O_{12}$ films, Å	FWHM of (444)$Lu_3Fe_5O_{12}$ reflection, deg.
YAG(111)	12.29(1)	0.22(1)
GAGG(111)	12.26(1)	0.17(1)
GGG(111)	12.26(1)	0.22(1)
NdGG(111)	12.26(1)	0.20(1)

defined character, which can also be interpreted as a consequence of high elastic compressive stresses (and, possibly, chemical interactions at the interface) while maintaining the epitaxial inheritance of the substrate structure by the film. Plotting the dependence of the FMR line width (ΔH) (Fig. 6b) on the mismatch value at the interface reveals a clear minimum for the $Lu_3Fe_5O_{12}$ film obtained on the GAGG(111) substrate: the least deformed film on this substrate exhibits the narrowest FMR line $\Delta H = 171(+/-8)$ Oe. Thus, among the substrates we have considered, $Gd_3(AlGa_4)O_{12}$ is more suitable than others for obtaining high-quality epitaxial $Lu_3Fe_5O_{12}$ films with a minimum FMR line width due to the smallest mismatch of parameters between the film and the substrate.

In the next stage of the study, $Lu_3Fe_5O_{12}$ films with thicknesses ranging from 45 to 800 nm were deposited on the surface of single-crystal GGG-substrates with (111) and (210) orientations, with growth on substrates of both orientations being performed in a single cycle. Deposition of all films was carried out under identical conditions ($T_{deposition}$, p_{total}, pO_2, V_{growth}), with only the deposition time varied to obtain films of different thicknesses. The results of X-ray phase analysis of the films on the GGG(111) substrate are shown in Fig. 7a. As can be seen from these data, the resulting films remain epitaxial at all thicknesses. However, a decrease in intensity and an increase in reflection width with increasing film thickness indicate a gradual accumulation of epitaxial layer defects. A noticeable shift in the reflection of the $Lu_3Fe_5O_{12}$ garnet film toward the value indicated by the "powder card" indicates that elastic stresses in the film, arising at the interface with the substrate, decrease as the epitaxial layer thickness increases, which is also demonstrated by the dependence of the unit cell parameters of the $Lu_3Fe_5O_{12}$ film on thickness (Fig. 7b). This pattern is entirely consistent with the classical behavior of thin-film heteroepitaxial structures. It should also be noted that reflections from secondary phases of α-Fe_2O_3 and o-$LuFeO_3$ appear in the X-ray diffraction patterns of 800 nm-thick films. Their origin is similar: with increasing film thickness, the orienting force of epitaxy weakens, and on the surface of the thickest films, phase formation during film deposition resembles a solid-phase reaction proceeding via a diffusion mechanism, with diffusion having a two-dimensional surface character. The completeness of the formation of the $Lu_3Fe_5O_{12}$ phase by the reaction of α-Fe_2O_3 with o-$LuFeO_3$ depends on the rate of surface diffusion, which decreases sharply as the film thickness increases with increasing surface roughness.

In the thinnest film (45 nm) on GGG(111), a weak reflection of the hexagonal phase *h*-$LuFeO_3$ is noticeable. This phase is thermodynamically unstable in the autonomous state, but is easily stabilized by minimizing the interface energy on

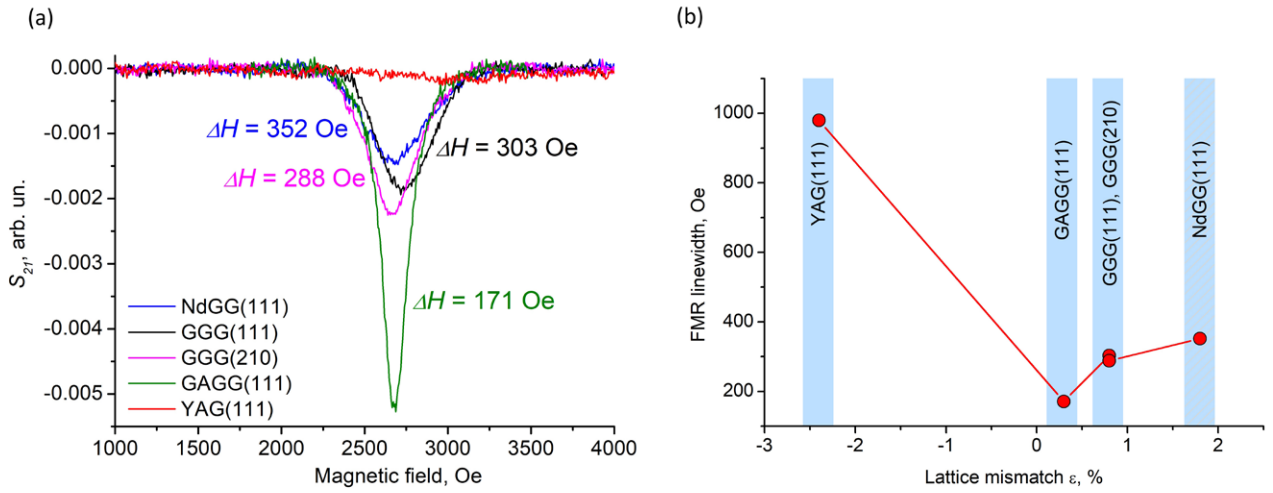

Fig. 6. (a) Comparison of FMR spectra (S_{21} – the absorption coefficient) of $Lu_3Fe_5O_{12}$(111) films on different substrates. Microwave frequency is 9 GHz. (b) Dependence of ferromagnetic resonance linewidth on the lattice mismatch of film/substrate

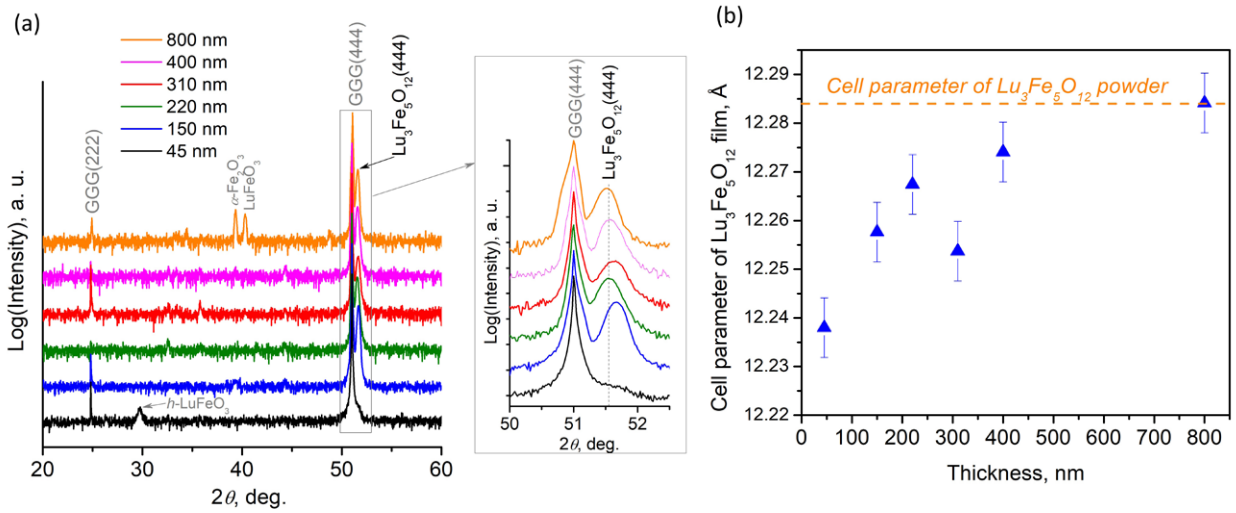

Fig. 7. (a) θ–2θ X-ray diffraction patterns of $Lu_3Fe_5O_{12}$ films of different thicknesses on a $Gd_3Ga_5O_{12}$(111) substrate. (b) Dependence of the unit cell parameters on the thickness of $Lu_3Fe_5O_{12}$ films on a $Gd_3Ga_5O_{12}$(111) substrate

surfaces with a hexagonal oxygen ion packing motif, which includes the (111) plane of garnet [31, 32]. The FMR measurement results presented in Fig. 8a and Fig. 8b demonstrate that ferromagnetic resonance is observed in all of the obtained films, with the exception of the 45 nm-thick films. Fig. 9 shows the obtained dependences of the FMR linewidth (ΔH) on the film thickness. These dependences, for films of both orientations, clearly show two distinct branches, characterizing two alternating stages of epitaxial growth. The descending branch (to the left of the minimum) at small thicknesses reflects the influence of epitaxial elastic stresses in the films arising from the difference in the UC- parameter at the boundary with the substrate, and the ascending branch (to the right of the minimum) indicates that in thicker films, due to the weakening of the orienting influence of the substrate, local disturbances of the crystalline order occur, and various extended defects accumulate (low-angle and high-angle boundaries, mosaicism, antiphase boundaries, etc.), i.e., a gradual transition to the growth of a polycrystalline layer occurs. The minimum ΔH(FMR) corresponds to films in which significant relaxation of epitaxial stresses has occurred, but the concentration of defects characteristic of the polycrystalline state is still low.

Further work toward producing $Lu_3Fe_5O_{12}$ garnet films with a narrower FMR linewidth

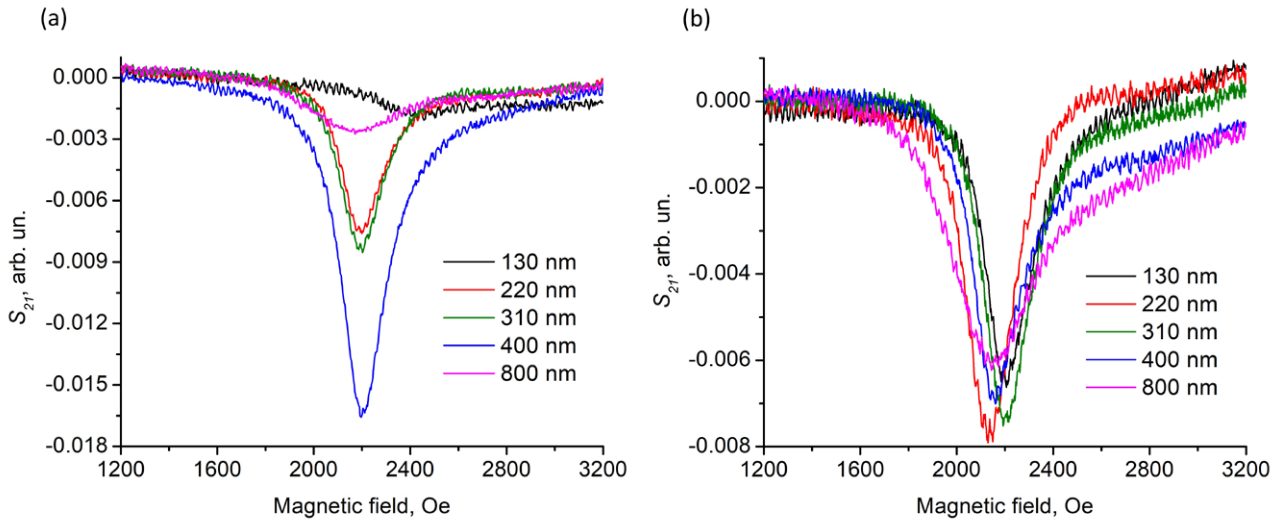

Fig. 8. FMR spectra of $Lu_3Fe_5O_{12}$ films of various thicknesses on $Gd_3Ga_5O_{12}$(111) (a) and $Gd_3Ga_5O_{12}$(210) (b) substrates. Microwave frequency is 9 GHz

requires a more detailed study of the influence of temperature and film deposition rate, taking into account the results of this paper.

4. Conclusions

$Lu_3Fe_5O_{12}$ films of varying thickness were synthesized for the first time using the MOCVD method on $Nd_3Ga_5O_{12}(111)$, $Gd_3Ga_5O_{12}(111)$, $Gd_3Ga_5O_{12}(210)$, $Gd_3(AlGa_4)O_{12}(111)$, and $Y_3Al_5O_{12}(111)$ substrates. X-ray diffraction (θ–2θ and ϕ-scanning) demonstrated the epitaxial nature of the films, and their magnetic properties were studied using ferrimagnetic resonance spectroscopy. A systematic study of the dependence of the FMR linewidth of $Lu_3Fe_5O_{12}$ on the mismatch between the unit cell parameters of the film and the substrate was performed for the first time. It was found that the minimum ΔH(FMR) of $Lu_3Fe_5O_{12}$ films is achieved on $Gd_3(AlGa_4)O_{12}$ substrates, which have a minimal mismatch between the unit cell parameters and the film. It has been shown that the dependence of ΔH(FMR) on film thickness is extreme, with the minimum corresponding to a film thickness at which significant relaxation of epitaxial stresses has occurred, but the concentration of defects characteristic of the polycrystalline state is still low. Taking these factors into account will enable the production of Lu-iron garnet films with a narrower ferromagnetic resonance linewidth, which could be used in various areas of spintronics as sensitive elements in microwave detectors.

Author contributions

A. A. Hafizov and R. Gu conducted the thin-film vapor-phase deposition experiments. M. N. Markelova developed the study concept, processed the X-ray diffraction data, and wrote the manuscript. I. E. Graboy developed the methodology and wrote the manuscript. V. A. Amelichev conducted the thin-film X-ray diffraction experiments. D. A. Volkov and D. A. Gabrielyan conducted the FMR absorption spectroscopy experiments and edited the manuscript. Safin A. R. – research concept, methodology development, text editing. Nikitov S. A. – scientific supervision, research concept, methodology development. Kaul A. R. – scientific supervision, research concept, methodology development, text editing.

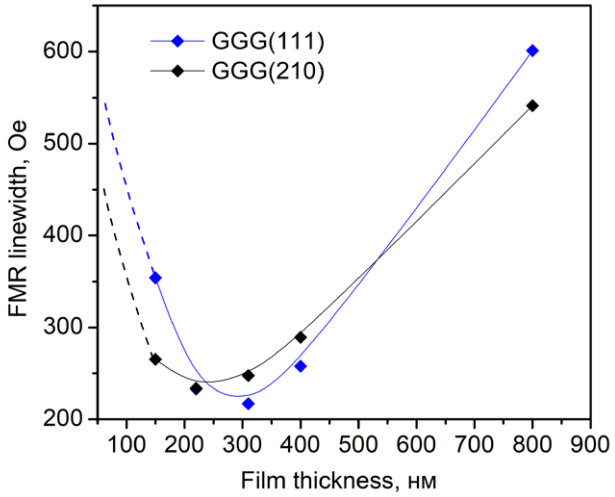

Fig. 9. Dependence of FMR linewidth on the $Lu_3Fe_5O_{12}$ film thickness on $Gd_3Ga_5O_{12}(111)$ and $Gd_3Ga_5O_{12}(210)$ substrates

Conflict of interests

The authors declare that they have no known competing financial interests or personal relationships that could have influenced the work reported in this paper.

References

1. Yang Y., Liu T., Bi L., Deng L. Recent advances in development of magnetic garnet thin films for applications in spintronics and photonics. *Journal of Alloys and Compounds*. 2021;860: 158235. https://doi.org/10.1016/j.jallcom.2020.158235

2. Borisenko V. E., Danilyuk A. L., Migas D. B. *Spintronics**. Laboratoriya znaniy Publ.; 2017. 229 p. (in Russ.)

3. Nikitov S. A., Kalyabin D. V., Lisenkov I. V… Pavlov E. S. Magnonics: a new research area in spintronics and spin wave electronics. *Physics-Uspekhi*. 2015;58: 1002–1028. https://doi.org/10.3367/UFNr.0185.201510m.1099

4. Žutić I., Fabian J., Das Sarma S. Spintronics: fundamentals and applications. *Reviews of Modern Physics*. 2004;76(2): 323–410. https://doi.org/10.1103/RevModPhys.76.323

5. Fert A. Nobel lecture: origin, development, and future of spintronics*. *Reviews of Modern Physics*. 2008;80(4): 1517–1530. https://doi.org/10.1103/RevModPhys.80.1517

6. Hirohata A., Yamada K., Nakatani Y., … Hillebrands B. Review on spintronics: principles and device applications. *Journal of Magnetism and Magnetic Materials*. 2020;509: 166711. https://doi.org/10.1016/j.jmmm.2020.166711

7. Chechenin N. G., Dzhun I. O., Babaytsev G. V., Kozin M. G., Makunin A. V., Romashkina I.L. FMR damping in thin films with exchange bias. *Magnetochemistry*. 2021;7(5): 70. https://doi.org/10.3390/magnetochemistry7050070

8. Geller S. Crystal chemistry of the garnets. *Zeitschrift für Kristallographie*; 1967;125: 1-47. https://doi.org/10.1524/zkri.1967.125.16.1

9. Liu C., Chen J., Liu T., … Wu M. Long-distance propagation of short-wavelength spin waves. *Nature Communications*. 2018;9(1): 738. https://doi.org/10.1038/s41467-018-03199-8

10. Zhu D., Zhao W. Threshold current density for perpendicular magnetization switching through spin-orbit torque. *Physical Review Applied*. 2020;13(4): 044078. https://doi.org/10.1103/PhysRevApplied.13.044078

11. Hahn C., de Loubens G., Klein O., Viret M., Naletov V. V., Ben Youssef J. Comparative measurements of inverse spin Hall effects and magnetoresistance in YIG/Pt and YIG/Ta. *Physical Review B*. 2013;87(17): 174417. https://doi.org/10.1103/PhysRevB.87.174417

12. Knauer S., Davídková K., Schmoll D., … Chumak A. V. Propagating spin-wave spectroscopy in a liquid-phase epitaxial nanometer-thick YIG film at millikelvin temperatures. *Journal of Applied Physics*. 2023;133(14): 143905. https://doi.org/10.1063/5.0137437

13. Jermain C. L., Paik H., Aradhya S. V., Buhrman R. A., Schlom D. G., Ralph D. C. Low-damping sub-10-nm thin films of lutetium iron garnet grown by molecular-beam epitaxy. *Applied Physics Letters*. 2016;109(19): 192408. https://doi.org/10.1063/1.4967695

14. Wu X., Wang X., Liu Y., … Zhu J. Study on dielectric and magnetodielectric properties of $Lu_3Fe_5O_{12}$ ceramics. *Applied Physics Letters*. 2009;95: 182903. https://doi.org/10.1063/1.3259651

15. Hou Y. Epitaxial growth and observation of the magnetodielectric effect in ferrimagnetic $Lu_3Fe_5O_{12}$ films. *Journal of Physics D: Applied Physics*. 2018;51(27): 275001. https://doi.org/10.1088/1361-6463/aac8d1

16. Hioki T., Hashimoto Y., Saitoh E. Bi-reflection of spin waves. *Communications Physics*. 2020;3: 188. https://doi.org/10.1038/s42005-020-00455-6

17. Volkov D. A., Gabrielyan D. A., Matveev A. A., … Nikitov S. A. Spin pumping from $Lu_3Fe_5O_{12}$. *JETP Letters*. 2024;119(5): 357–362. https://doi.org/10.1134/S0021364024600150

18. Dubs C., Surzhenko O. Magnetically compensated nanometer-thin Ga-substituted yttrium iron garnet (Ga:YIG) films with robust perpendicular magnetic anisotropy. *Advanced Electronic Materials*. 2025;11(15): e00232. https://doi.org/10.1002/aelm.202500232

19. Arsad A. Z., Zuhdi A. W. M., Ibrahim N. B., Hannan M. A. Recent advances in yttrium iron garnet films: methodologies, characterization, properties, applications, and bibliometric analysis for future research directions. *Applied Sciences*. 2023;13(2): 1218. https://doi.org/10.3390/app13021218

20. Yakovlev Yu. M., Gendelev S. Sh. *Iron ferrites monocrystals in radioelectonics**. "Sovetskoye Radio" Publ.; 1975. 360 p. (in Russ.)

21. Yushchuk S. I. Layered structure of epitaxial yttrium iron garnet films. *Technical Physics*. 1999;44: 1454–1456. https://doi.org/10.1134/1.1259547

22. Prokopov A. R., Vetoshko P. M., Shumilov A. G., … Belotelov V. I. Epitaxial Bi–Gd–Sc iron-garnet films for magnetophotonic applications. *Journal of Alloys and Compounds*. 2016;671: 403–407. https://doi.org/10.1016/j.jallcom.2016.02.036

23. Soumah L., Beaulieu N., Qassym L., … Anane A. Ultra-low damping insulating magnetic thin films get perpendicular. *Nature Communications*. 2018;9(1): 3355. https://doi.org/10.1038/s41467-018-05732-1

24. Yamahara H., Feng B., Seki M., … Tabata H. Flexoelectric nanodomains in rare-earth iron garnet thin films under strain gradient. *Communications Materials*. 2021;2: 95. https://doi.org/10.1038/s43246-021-00199-y

25. Khurana B., Kaczmarek A. C., Chou C.-T., … Ross C. A. Rare earth iron garnet superlattices with sub-unit-cell composition modulation. *ACS Nano*. 2024;18(52): 35269–35275. https://doi.org/10.1021/acsnano.4c11117

26. Ahamed E. I., Sarker M. S., Yamahara H., … Tabata H. Spin wave perturbation in rare-earth iron garnet thin films with epitaxial strain relaxation. *APL Materials*. 2025;13: 041114. https://doi.org/10.1063/5.0257413

27. Krichevtsov B. B., Gastev S. V., Suturin S. M., … Sokolov N. S. Magnetization reversal in YIG/GGG(111) nanoheterostructures grown by laser molecular beam epitaxy. *Science and Technology of Advanced Materials*. 2017;18(1): 351–363. https://doi.org/10.1080/14686996.2017.1316422

28. Samoilenko K. D., Volkov D. A., Gabrielyan D. A., … Nikitov S. A. Spintronic detector of linearly polarized microwave radiation based on a ferromagnet/normal metal heterostructure. *JETP Letters*, 2025;121(7): 554–561. https://doi.org/10.1134/S002136402460530X

29. Markelova M. N., Hafizov A. A., Shi X., … Kaul A. R. Chemical vapor deposition of $Tm_3Fe_5O_{12}$ epitaxial films, investigation of their structure and properties in the terahertz range. *Condensed Matter and Interphases*. 2025;27(1): 104–114. https://doi.org/10.17308/kcmf.2025.27/12488

30. Popova E., Keller N., Jomard F., … Tessier M. Exchange coupling in ultrathin epitaxial yttrium iron garnet films. *The European Physical Journal B - Condensed Matter*. 2003;31: 69–74. https://doi.org/10.1140/epjb/e2003-00010-2

31. Bossak A., Graboy I., Gorbenko O., … Zandbergen H. W. XRD and HREM studies of epitaxially stabilized hexagonal orthoferrites $RFeO_3$ (R = Eu–Lu). *Chemistry of Materials*. 2004;16(9): 1751–1755. https://doi.org/10.1021/cm0353660

32. Kaul A. R., Nygaard R. R., Ratovskiy V. Yu., Vasiliev A. L. TSF-MOCVD – a novel technique for chemical vapour deposition on oxide thin films and layered heterostructures. *Condensed Matter and Interphases*. 2021;23(3): 396–405. https://doi.org/10.17308/kcmf.2021.23/3531

* *Translated by author of the article*

Information about the authors

Abduvosit A. Hafizov, graduate student at the Higher School of Material Science, Lomonosov Moscow State University (Moscow, Russian Federation).

https://orcid.org/0009-0003-0740-8180

abduvosithafizov220@gmail.com

Maria N. Markelova, Cand. Sci. (Chem.), Research Fellow at the Department of Chemistry, Lomonosov Moscow State University (Moscow, Russian Federation).

https://orcid.org/0000-0002-1014-9437

maria.markelova@gmail.com

Ruoxuan Gu, master degree student at the Higher School of Material Science, Lomonosov Moscow State University (Moscow, Russian Federation).
https://orcid.org/0009-0006-5998-2194
grxuan969@outlook.com

Igor E. Graboy, Cand. Sci. (Chem.), Senior Research Fellow at the Department of Chemistry, Lomonosov Moscow State University (Moscow, Russian Federation).
https://orcid.org/0009-0003-7011-2200
graboi@inorg.chem.msu.ru

Vadim A. Amelichev, Cand. Sci. (Chem.), Technical Director at S-Innovations (Moscow, Russian Federation).
https://orcid.org/0000-0003-0886-9854
mailto:vadim.amelichev@gmail.com

Dmitry A. Volkov, Junior Researcher at the Kotelnikov Institute of Radio Engineering and Electronics, Russian Academy of Sciences; Assistant at Moscow Power Engineering Institute (Moscow, Russian Federation).
https://orcid.org/0009-0004-1655-8348
d.a.volkov.work@gmail.com

David A. Gabrielyan, Junior Researcher at the Kotelnikov Institute of Radio Engineering and Electronics, Russian Academy of Sciences; Assistant at Moscow Power Engineering Institute (Moscow, Russian Federation).
https://orcid.org/0000-0003-0801-0134
davidgabrielyan1997@gmail.com

Ansar R. Safin, Dr. Sci. (Phys.–Math.), Leading Researcher, Head of the Laboratory, Kotelnikov Institute of Radio Engineering and Electronics of the Russian Academy of Sciences; Professor, Moscow Power Engineering University; Professor, Moscow Institute of Physics and Technology (National Research University); Professor, National Research University Higher School of Economics (Moscow, Russian Federation).
https://orcid.org/0000-0001-6507-6573
arsafin@gmail.com

Sergey A. Nikitov, Dr. Sci. (Phys.–Math.), Acting Director, Head of Laboratory, Kotelnikov Institute of Radio Engineering and Electronics of the Russian Academy of Sciences; Head of Department, Moscow Institute of Physics and Technology (National Research University) (Moscow, Russian Federation); Head of Laboratory, N. G. Chernyshevsky Saratov National Research State University (Saratov, Russian Federation); Academician, Russian Academy of Sciences (Moscow, Russian Federation).
https://orcid.org/0000-0002-2413-7218
nikitov@cplire.ru

Andrey R. Kaul, Dr. Sci. (Chem.), Full Professor at the Chair of Inorganic Chemistry, Lomonosov Moscow State University, Moscow, Russian Federationю
https://orcid.org/0000-0002-3582-3467
arkaul@mail.ru

Received November 19, 2025; approved after reviewing December 1, 2025; accepted for publication December 15, 2025; published online April 01, 2026.